Position reconstruction in fission fragment detection using the low pressure MWPC technique for the JLab experiment E02-017 *

QIU Xi-Yu(邱玺玉)[1] L. Tang[2,3] A. Margaryan[4] XU Jin-Zhang(徐进章)[1,5]
HU Bi-Tao(胡碧涛)[1] CHEN Xi-Meng(陈熙萌)[1;1)]

[1] School of Nuclear Science and Technology, Lanzhou University, Lanzhou 730000, China
[2] Department of Physics, Hampton University, Hampton, VA 23668, USA
[3] Thomas Jefferson National Accelerator Facility, Newport News, VA 23606, USA
[4] Yerevan Physics Institute, Yerevan 375036, Armenia
[5] School of Electrical and Automation, Hefei University of Technology, Hefei 230009, China

Abstract: When a Λ hyperon is embedded in a nucleus it can form a hypernucleus. The lifetime and its mass dependence of stable hypernuclei provide information about the ΛN interaction in the nuclear medium. This work will introduce the Jefferson Lab experiment (E02-017), which aims to study the lifetime of the heavy hypernuclei using a specially developed fission fragment detection technique: a multi-wire proportional chamber operating under low gas pressure (LPMWPC). The trajectory of the detected fragment is reconstructed and used to find the fission point on the target foil, the position resolution is less than 1 mm, which meets the original design, the separation of target materials and events mixture percentage in different regions are verified by Monte Carlo simulation.

Key words: hypernuclei, decay, LPMWPC, fission fragment, position reconstruction

PACS: 29.90.+r **DOI:** 10.1088/1674-1137/38/7/074003

1 Introduction

Since its discovery in 1952 [1], the Λ hypernuclei (in which one of the nucleons in the nucleus is replaced by a Λ hyperon) has been studied very extensively. One of this study's interests is the weak decay of the Λ hypernuclei. Generally, most of the produced Λ hypernuclei stand in their excited states and they can then reach the ground state by emitting a nucleon or through electromagnetic decay[2]. At ground state, the Λ hypernuclei decays via δS=1 weak interactions.

In free space, a Λ hyperon decays only via mesonic weak decay into a nucleon and a pion:

$$\Lambda \rightarrow \mathrm{p}+\pi^- + 37.8\ \mathrm{MeV}\ (B.R.\approx 63.9\%), \quad (1)$$

$$\Lambda \rightarrow \mathrm{n}+\pi^0 + 41.1\ \mathrm{MeV}\ (B.R.\approx 35.8\%), \quad (2)$$

when the Λ hyperon is embedded into a nucleus, which forms a hypernuclei, it will decay via two different channels: mesonic decay and non-mesonic weak decay. Since there is about 40 MeV of released energy (mass difference between the Λ mass and the summed mass of the pion and nucleon) during the mesonic decay mode, it is too small to make the decay nucleon (proton or neutron) escape from the nucleus of the s orbit. These channels are significantly suppressed as the hypernuclear mass increases. Therefore, the non-mesonic decay mode becomes a dominant decay channel for the hypernuclear. This kind of decay also has three sub-channels:

proton induced:

$$\Lambda+\mathrm{p}\rightarrow \mathrm{n}+\mathrm{p}+176\ \mathrm{MeV}\ (B.R.-\Gamma_\mathrm{p}); \quad (3)$$

neutron induced:

$$\Lambda+\mathrm{n}\rightarrow \mathrm{n}+\mathrm{n}+176\ \mathrm{MeV}\ (B.R.-\Gamma_\mathrm{n}); \quad (4)$$

three body decays:

$$\Lambda+\mathrm{N}+\mathrm{N}\rightarrow \mathrm{n}+\mathrm{N}+\mathrm{N}+176\ \mathrm{MeV}\ (B.R.-\Gamma_2); \quad (5)$$

where N is either a p or an n.

The 176 MeV released energy is simply the mass difference between Λ and decay nucleon, and it is sufficiently large for the nucleon to escape from the nucleus. Therefore, in contrast to mesonic decay, the non-mesonic decay quickly becomes dominant as mass increases. For heavy hypernuclei, the non-mesonic decay can also trigger nuclear fission or fragmentation. Therefore, time delayed fission contains characteristics of the non-mesonic weak decay of heavy hypernuclei. Based on this idea, the COSY-13 collaboration has studied the lifetime of the heavy Λ hypernuclei produced by proton interaction with

Received 29 September 2013
∗ Supported by National Natural Science Foundation of China (11175075, 11135002 and 91026021)
1) E-mail: chenxm@lzu.edu.cn

Au, Bi and U nuclei using a recoil shadow method [3–5]. In this method, the lifetime is converted from the position distribution in the shadow region, that only fragments with time delayed decay can reach. However, the conversion depends on the modeling of the momentum and mass distributions of decay hypernuclei. The resulting lifetime is quite short, ∼145 ps, and could not be explained by current theories on baryonic weak interactions.

The Jefferson Lab experiment E02-017, using a photo-production (γ, K^+) reaction to produce Λ hypernuclei, aims to directly measure the lifetime of these heavy hypernuclei by utilizing the same time delayed fission characteristics as COSY-13 did, while applying the low pressure MWPC technique developed in detecting both the time and position of fission fragments. Multiple target materials are spotted as strips on a single thin Mylar foil in order to simultaneously produce hypernuclei with different masses. The production rate from different targets depends on the Gaussian type of spread of the photon beam intensity distribution. This work will give a brief introduction to the experimental setup and will present the method of the fission position reconstruction on the target, and the target separation result will be given.

2 Experiment

The Jefferson Lab experiment E02-017 was carried out in Experimental Hall C parasitically with the hypernuclear mass spectroscopy experiment E05-115. The entire experimental setup is illustrated in Fig. 1.

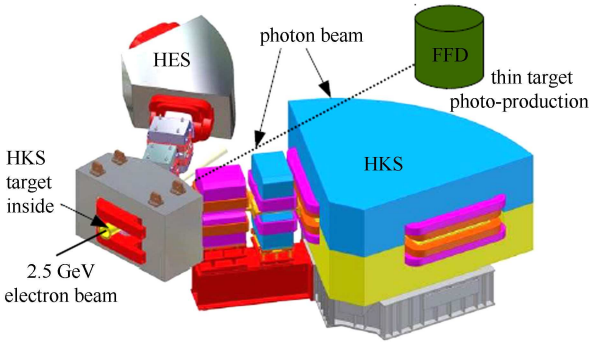

Fig. 1. (color onlie) The experimental setup for E05-115 and E02-017 in JLab Hall C.

The Jefferson Lab accelerator provides a high quality continuous wave (CW) electron beam, which has 1.67 ps pulse width and 2 ns pulse separation. The beam energy used by E05-115 is 2.5 GeV. The electron beam hit the E05-115 target that was located at the entrance of the splitter magnet which bent the oppositely charged scattered electrons and K^+s to the HES (e′) and HKS (K^+) spectrometers, respectively. The post beam is also bent and is aimed directly at the electron beam dump. The real bremsstrahlung photons produced from the E05-115 target are not affected by the splitter magnet and go straight forward to the local photon dump, which is about 15 meters downstream the E05-115 target along the incoming beam direction. This dumped photon beam is utilized as a real photon beam with a wide range of beam energy up to 2.5 GeV for the E02-017 experiment, which is set up just in front of the local photon dump. The threshold photon energy to produce Λ hyperon is about 700 MeV.

The entire experimental system of the E02-017 is contained in one common low pressure chamber, which is filled with pure heptane gas whose pressure is regulated at about 400 Pa. A thin tilted target foil is located at the center of the chamber and aligned to intercept the incoming photon beam. The fission fragment detector (FFD) system used for E02-017 is symmetrically allocated above and below the tilted target foil.

The FFD is specially developed for this experiment and based on the low pressure multi-wire proportional chamber (LPMWPC) technique [6, 7]. The detector has a modular structure and contains four independent LPMWPC units. Two units are above the target foil, forming the top telescope and time-of-flight (TOF) pair, and two units are placed below the target foil to form the bottom pair. The top and bottom pairs are completely symmetric and all of the detector planes are parallel to the beam direction.

Each LPMWPC unit consists of one central anode wire plane (A) at a potential of +300 V, two cathode wire planes (C) at a ground potential that sandwiches the anode plane, and two guard planes (G) at a potential of −100 V that are placed further outside the cathode planes. Thus, each unit has symmetric G-C-A-C-G plane order. The A plane is formed by 12 μm gold-plated tungsten wires with 1 mm spacing. The wires are electrically connected together to provide a single timing signal when detecting one passing fragment. The C planes are formed by 40 μm gold-plated tungsten wires, which also have 1 mm spacing. However, the wires are electrically grouped by three wires and each group is connected to one tab of the digital delay line chip with 2 ns delay between two adjacent tabs. A chain of digital delay line chips are mounted on one side of the board. Induced charges at a specific wire group give two signals traveling through the delay line chains in two directions: to the left (L) and to the right (R). The timing is analyzed in reference to the same A plane timing. The time difference, L−R, provides position information while the time sum, L+R, can be used to filter the noise and multiple fragment detection, and can be used to estimate the position resolution (or uncertainty). The two cathode

planes have wires that are laid normal (90°) to each other dimensional position can be so that the two determined for single detection point by each unit while the A plane provides the detection time. The two G planes provide the second step ionization to increase the signal size and set an equal potential between units to minimize noise charges. The plane separation is 3.175 mm. The two outer units have an active area of 21 cm×21 cm while that for the inner two units is 10.5 cm×10.5 cm. The vertical distance between the beam line centroid to the inner A plane is 3 cm and that between the two A planes of the inner and outer units is 7 cm. Therefore, the detection of fission fragment at any unit includes information of time (T) and three dimensional positions (X, Y, Z). In our FFD geometry definition, X is in beam direction, Y is normal to X and parallel to the LPMWPC planes, and Z is normal to both beam and LPMWPC planes. T is measured relative to the event trigger time. All of the measured parameters are labeled 1–4 from the bottom unit upward. Since no particle from production process is available, the time signal from the bottom outer A plane is used as time reference for all events and, therefore, $T1$ is always a constant. Under low gas pressure, the ionized particles have a long free mean path length. The gas gain is very low in comparison with the conventional MWPC or drift chambers. Thus, only fission fragments with high Z can produce signals with sufficient pulse size. Low mass and low Z fragments or particles cannot be detected. Since the signal is still at least 10 times smaller than that from regular MWPC, each signal is pre-amplified by 100 times with a fast pre-amplifier mounted on the edge of the associated wire plane. The analog signals are then extracted outside of the vacuum sealed chamber and again amplified 10 times before being converting to logical signals. More detailed description of this FFD can be found in Refs. [6, 7].

The target used in the experiment is made by spotting various materials onto a 2.0 μm thick aluminized mylar foil, which is located at the center of the two arms. The mylar functions as the backing and is stretched over a rectangular aluminum ring frame with an active area of 13.2 cm×8.2 cm. The Fe target is specially prepared in order to make consistency verification with the previous measurements done by KEK group on $_{\Lambda}$Fe results. The target frame is placed in a small incline angle (10 degrees) with respect to the beam direction in order to maximize the target thickness for the beam photons in X-direction (i.e. to increase the production rate) while minimizing the thickness for the escaping fission fragments towards the LPMWPCs (i.e. to maximize the fragment escaping rate).

Table 1 lists all of the materials prepared for the experiment, the thickness, and the actual separations between materials. The list follows the same sequence as the material arrangement on the backing foil and Fe material is at the center with respect to the beam. The small incline angle allows the photon beam with narrow angular distribution to cover a wider range of target materials. However, the sharp beam distribution still does not allow productions from Au and U targets. Thus, data are collected only from the four targets closer to the beam center. In addition, 2.5 mm separation was originally planned between target regions but the masking difficulty during the sputtering process made smaller and uneven separations. In the case of Cu and Au, the mask completely failed. This will be discussed in more detail later in the events separation section.

Table 1. Target materials used in the experiment.

target	thickness/μm	width/mm	separation/mm
Au	0.4	29.0	0.0
Cu	0.8	25.5	2.0
Fe	0.8	20.0	1.0
Ag	0.8	21.5	1.0
Bi	0.4	20.0	1.5
$U_{natural}$	<0.003	11.5	

In addition, a ^{252}Cf spontaneous fission source is mounted in a source holder with a collimator at a distance of 13.73 cm away from the anode plane of the top unit. The fission fragments that have escaped from the source were used to test FFD. The source test results and characteristic performance without target foil and beam can be found in Ref. [6]. During the experiment, the source events are also used to check the condition of the FFD. However, the three extra foils (i.e. the target foil and the two beam induced charge separation foils made by the same 2 μm aluminum Mylar) made a significant difference between the velocities measured by the top pair and bottom pair of LPMWPCs due to energy loss, which is a function of momentum. Therefore, under experimental condition with foils inserted, the fragments from the source are only used to check basic operational conditions and alignment calibration. The structure and geometry of FFD discussed above is schematically illustrated in Fig. 2.

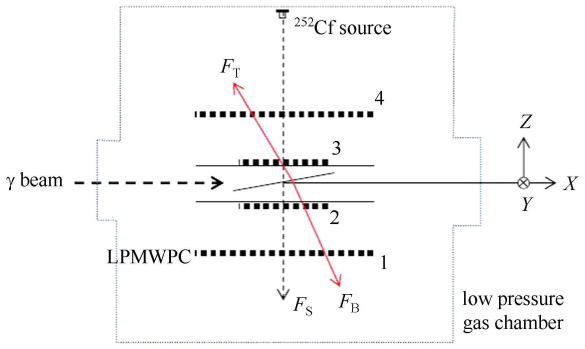

Fig. 2. (color online) Schematic illustration of the structure and geometry of FFD.

3 Position reconstruction method and result

The position where a fragment passes through a LPMWPC unit is determined by using the induced signals detected from the C planes, as mentioned in the previous section. The delay line technique [8, 9] is applied so that each charge induction at a detection LPMWPC unit splits into two pulse signals in opposite directions. This pair of signals is converted into two times (for instance, XiL and XiR while i=1–4 is the LPMWPC unit number) by time-digital-conversion (TDC) in reference to the anode (A) plane signal time. Then, the detected position is determined by, for example, $Xi=F\times(Xi\mathrm{R}-Xi\mathrm{L})$ in X direction on the i^{th} unit with R is in the positive beam direction. Here, F is the time to length conversion factor, which is simply the total delay line time divided by the total C plane width. This needs to be calibrated when taking into account the TDC conversion factor and the precision of delay line chips. The sum of XiR and XiL (i.e. $SXi=Xi\mathrm{R}+Xi\mathrm{L}$) is also an important parameter. First of all, SXi for single fragment detection should be a constant. Therefore, a tight gate in the analysis to select the events in the sharp peak appearing in the SXi distribution can be a powerful cut to eliminate the background and mixing of multiple fragments. Secondly, SXi can be used to evaluate the position resolution since the uncertainty is at the same level for both ($Xi\mathrm{R}+Xi\mathrm{L}$) and ($Xi\mathrm{R}-Xi\mathrm{L}$). Position reconstruction and the geometry alignment are verified by checking the tracking of the fragments emitted from the calibration ^{252}Cf source mounted at the top, as illustrated in Fig. 2. With the same analysis cuts as used above, events with single fragment penetrating through all four units are selected. The peak width of the single plane residuals, which are obtained by fitting a straight line from the four measured X positions, is about 1 mm for all four units, see Fig. 3.

This is expected to be worse than the first test result in Ref. [6] since the two charge separation foils and a target foil were then inserted for the experiment. The fragments from the ^{252}Cf source must penetrate all three foils in order to reach the bottom pair of LPMWPCs. The significant energy loss and multiple scatterings increase the residuals from a straight line fit. Since the geometric information from the two dimensional X-Z planes is sufficient to make TOF reconstruction, no analysis is made in Y direction.

With the beam on target it is anticipated that a large amount of low energy electrons induced by the beam may be piled in the target region, whose density decreases as inversed square distance. This charge background does not generate signals to be detected as fragments but reduces the electric potential between the C and A planes of LPMWPC. Therefore, the two inner units, which have their A planes only 3 cm away from the beam center line, are expected to have less efficiency and worse single plane position resolution, that is, a large time jitter in the signals for XiR and XiL, which are used to find the position on the i^{th} plane. This is checked by the sum of left and right delay time (i.e. $Xi\mathrm{R}+Xi\mathrm{L}$), as discussed previously. Fig. 4 shows this sum for each of the X planes.

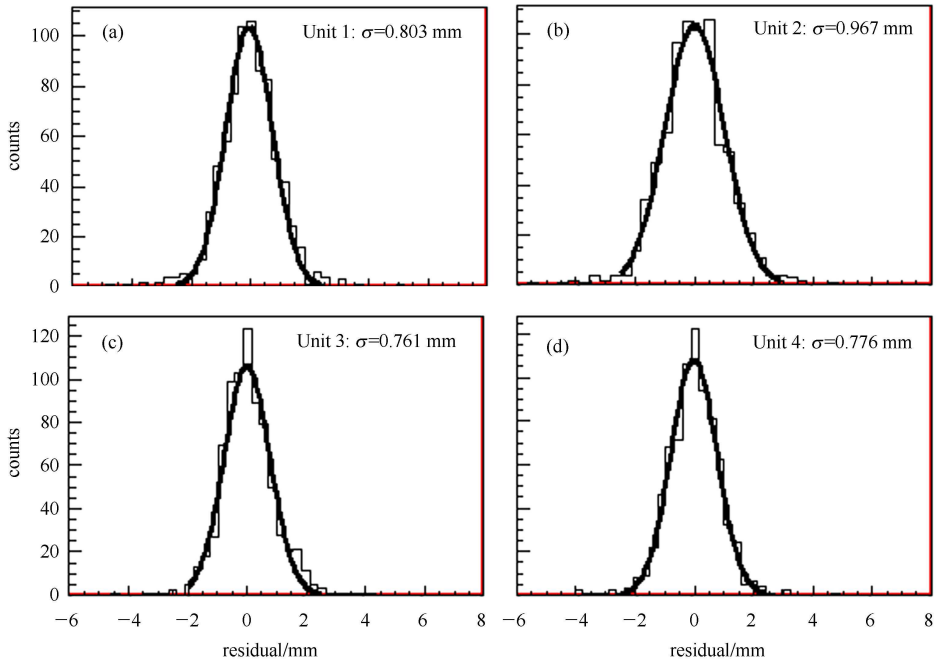

Fig. 3. (color online) The single plane residuals of the four X planes.

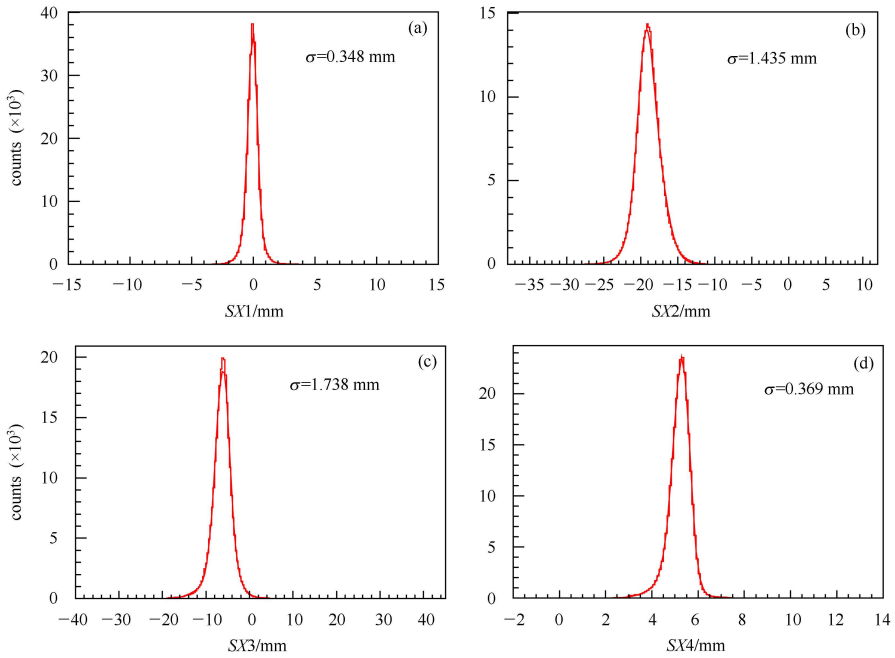

Fig. 4. (color online) Sum of the left and right delay time for each X plane in the associated LPWMC units. $SX1$ and $SX4$ are the planes in the outer two units while $SX2$ and $SX3$ in the two inner units which are close to the beam (see Fig. 2).

The two outer X planes have a position resolution of 0.35–0.37 mm. This agrees with the conclusion from the source study in Ref. [6]. Since they are 10 cm away from the beam, the piled charge effect is almost negligible. However, the inner units are affected by this charge pile up obviously and significantly. The position resolution deteriorated to about 1.44 mm and 1.74 mm for Unit 2 (just below the beam) and Unit 3 (just above the beam), respectively. The poor position resolution of the inner units meant that the separation of the target materials was not done cleanly. Therefore, a Monte Carlo simulation is necessary in helping to obtain the possible mixing percentages for the events from the adjacent target regions.

3.1 Monte Carlo simulation

In the Monte Carlo simulation, binary fission at its center of mass (CM) is assumed without lifetime. The statistical distribution of the total kinetic energy is based on the measured quasi-free mass distribution in the kinematics acceptance corrected spectrum of the $^{28}_{\Lambda}$Al hypernuclei obtained by the electro-production (JLab experiment E01-011) at small forward electron scattering angles. The change of distribution for heavier hypernuclei is assumed not to affect the simulation for position reconstruction study.

The two simulated fission fragments are generated from the target foil based on the target material regions with the measured gaps between regions. An emission

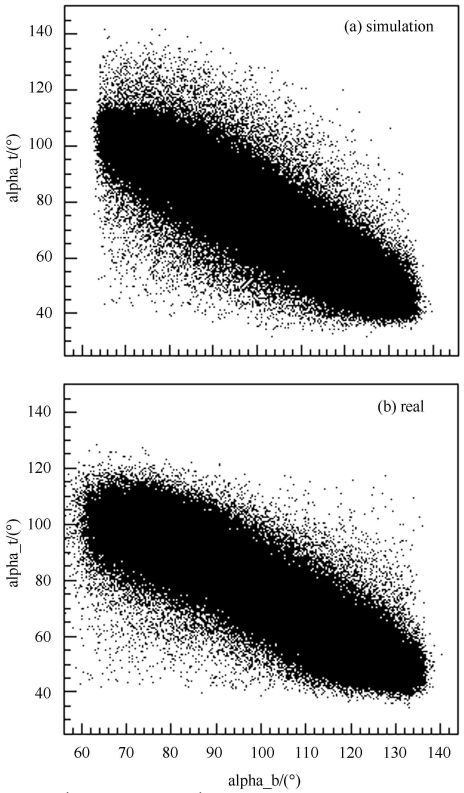

Fig. 5. (color online) Emission angle correlation between the two detected fragments, (a) is generated by Monte Carlo while (b) is from the real data. The density of the distribution represents the probability.

angle with respect to the beam direction ($+X$) is generated for each of the two fragments from one fission event, using a three dimensional Monte Carlo with the probability obtained from the real measurement. Fig. 5(a) shows the correlation between the emission angles of the two simulated fragments while Fig. 5(b) is that from the real experimental measurement, which is also used to extract the probability distribution function. The actual active area size of the LPMWPC units has an effect on the boundary shape. General agreement is sufficient for the purposes of the simulation study.

The sum of the two emission angles is the opening angle between the two fragments. The distribution in red color in Fig. 6 shows the distribution of the measured opening angles. The blue colored distribution is that from the simulated events. Good agreement can be seen by comparing these two distributions. Single plane position resolution has a small effect, mainly on the shaping in the tails of the opening angle distribution.

The simulation simply used the extracted probability functions from the real measurement without identification of their physics origins. However, one feature from the opening angle distribution can be easily seen. If CM of fission is at rest, then the two fragments from a pure binary fission should be emitted back to back; that is, with an opening angle of 180°. Position resolution of the LPMWPC units can broaden the opening angle distribution for only a few degrees, according to the geometry. Due to momentum transfer in the photo-reaction, CM of fission has momentum, which boosts the two fragments slightly forward in the direction of the beam. Including the range (250–500 MeV/c) of 3-momentum transfer in photoproduction of heavy hypernuclei, the opening angle of binary fissions is found to be centered at 177°, and this agrees well with that from the measurement, but the range is still small. It is commonly known that 2 to 10 nucleons can be emitted during the fission of heavy nuclei. However, the tail of the opening angle distribution is extended about 40° beyond the simulation that includes the nucleon emissions. This indicates two additional possible fission processes. The first is from the one-step fissions that have multiple ($\geqslant$2) fragments with only two detected within the acceptance. The second is from events experiencing two-step fissions. In a case of heavy hypernuclei, the initially excited hypernuclei can have masses above nuclear break-up thresholds, so that they decay first via break up reaction that emits a fragment to be stabilized into lighter hypernuclei (i.e. hyperfragments). The lighter hypernuclei then decay via a non-mesonic weak decay by emitting two nucleons and a nucleus in the process. Thus, the two fragments in this case are not from the same kinematic reaction. This reaction is the source in this experiment to study the lifetime of hyperfragment and this part will not be discussed in this paper. The two Monte Carlo generated fragments have their positions calculated at the LPMWPC units according to their geometry. To study the effect from the position uncertainty, the single plane position resolution is assumed to be that from the corresponding SXi=XiR+XiL (see Fig. 4). However, it is noticed that the peaks are not perfectly symmetric, especially in the tail regions, and could not be perfectly fitted by a single Gaussian function including the full tails. In fact, the measured XiR and XiL originate from the same induced charges but travel through two parts of the total delay line. Statistically, SXi shows the same average uncertainty as that of Xi=XiR−XiL. But SXi and Xi can have different asymmetry and tail distribution. Therefore, additional information is needed to obtain more realistic single plane resolution function for simulation purposes.

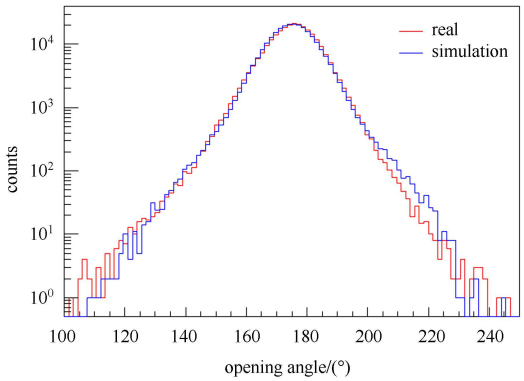

Fig. 6. (color online) Distribution of the opening angles between two detected fragments. Histogram in red is from real data while the simulation is in blue.

The position on the target in X direction is reconstructed separately by the two fragments detected by the top and bottom pairs. The difference (ΔX) between the two reconstructed X values ($X_{\rm top}$ and $X_{\rm bottom}$) is the only available additional information that can be used to study the single plane resolution, as shown in Fig. 7. Its shape is defined by the FFD geometry and reconstruction to a tilted target foil but its asymmetry contains contributions from the asymmetry tail shape of the single plane resolution function of the four LPMWPC units. On the other hand, a large ΔX does not mean a large error in determining the fission position since the fission position is decided by the mean of the $X_{\rm top}$ and $X_{\rm bottom}$. Uncertainty of the reconstructed fission position is determined by the uncertainty of $X_{\rm top}$ and $X_{\rm bottom}$. In Fig. 7, the distribution in red color is from the real data while the blue one is from the simulation. The initial position resolution function for each LPMWPC unit is extracted from SXi using three Gaussian fit. The main disagreement is the asymmetrical shape in the tail region. The resolution

function for each unit is then adjusted based on the level of sensitivity to the shape of this distribution. The final simulation result (shown in blue color) still has a small residual disagreement in the tails but contains less than 3% of events. This small disagreement might come from other unknown factors. The current level of simulation is sufficient to study the fission position reconstruction and mixing of the events from adjacent target regions after region separation.

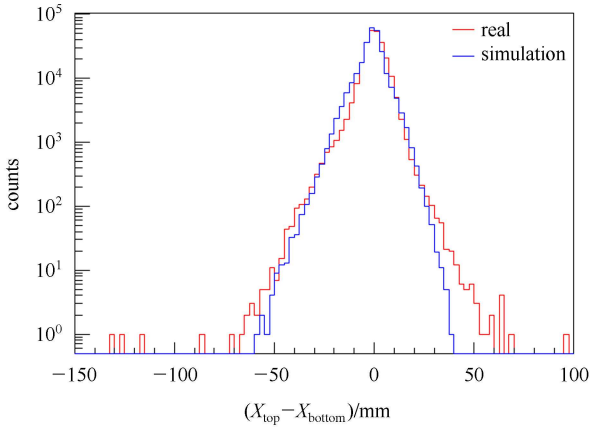

Fig. 7. (color online) The difference between the target position in X direction reconstructed by the top and bottom pairs of LPMWPC units.

3.2 Fission position reconstruction

The fission position on the target, projected to X direction, is reconstructed by solving the intersection of the trajectory of the fragment and the target plane. This position is reconstructed separately by the fragments detected by the top and bottom pairs of the LPMWPC units. The average of these two is used as the fission position on the target.

In Fig. 8, the distribution with red color is the reconstructed fission position. The mean separation boundary of the target regions is marked by the straight lines with target material labeled. Events from the Au and U materials are too rare thus, they are not labeled but their information can be found in Table 1.

It is obvious that this reconstruction distribution does not show gaps or "dips" that indicate the material separations. This makes the X coordinate alignment difficult to verify. It also means that the mixture of events from different target materials is unavoidable. Thus, simulation is needed to verify that the absence of gaps or "dips" that result from limited position resolution, as discussed previously, and to provide an estimation of the percentage event mixing, which must be taken into account when lifetime is extracted from the decay time spectrum after events separation.

The shape of this fission position distribution is dominantly determined by the photon beam intensity profile in the plane normal to the beam direction. Although fission probability increases as target mass increases, its effect is too small in competing with the sharp falling intensity of the beam. Thus, fission probability variation is not considered separately in the simulation.

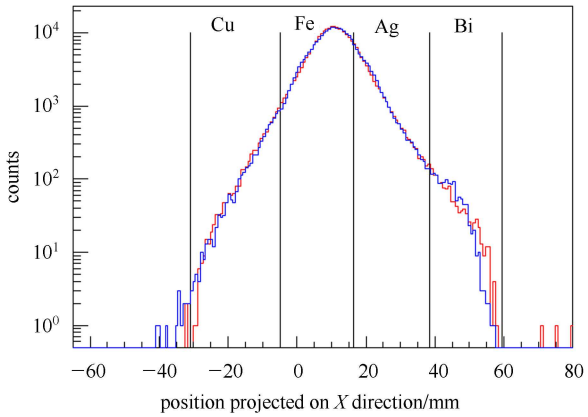

Fig. 8. (color online) The reconstructed fission position on target (projected in X direction). The distribution in red is from real data while that in blue is from simulation.

Although the electron beam energy used by the hypernuclear mass spectroscopy experiment E05-115 is almost monochromatic, the photons radiated from its target have a full range of energy, up to its maximum. The angular distribution of Bremstrahlungs varies according to the photon energy. Therefore, the intensity distribution is not expected to be able to be described precisely by a single Gaussian function: it has significant tail distribution. In addition, the radiated photon beam is transmitted within a vacuum pipe with a small diameter. A small emission angle misalignment for this experiment is observed by the asymmetry of the counting rate and efficiency between the top and bottom LPMWPC units. This is due to the tuning for the specific beam position by the experiment E05-115 for the optimized beam position on its target, which is the radiator for this lifetime experiment E02-017. This misalignment caused background photons from scatterings in the beam pipe material. On the other hand, the beam spread could help to enlarge the photon beam profile size, so that more target materials could be in the beam simultaneously. Therefore, it is accepted. Therefore, such asymmetric distribution is expected. Unfortunately, the E05-115 target is so thin that the radiation length is too short to spread the photon beam further to have events at least from the Au target. The U target material is too thin to be considered.

The distribution is fitted by using a function that contains four Gaussian functions, which allows different means and widths. The extracted beam profile function gives a continued distribution with its full tails. The

function is used as the probability function in the simulation in generating fission events from target foil according to its realistic geometry. No material is assumed in the U region. The distribution in blue color in Fig. 8 is the reconstructed fission position from the simulated events.

This is obvious for the sharp cut-off for the number of events at the U boundary. No significant amount of events could be obtained from the Au target. Indeed, it has been verified that only Cu, Fe, Ag and Bi have a sufficient number of events for the later lifetime study. Also, with the obtained single plane resolutions, no "dips" could be seen from the simulated events.

To find a positive signature that can further verify the X alignment (besides the U boundary), a ΔX gate is studied, hoping to select events with better position resolution. Fig. 9 shows the resulted fission position distribution from events within an extremely tight gate, -0.1 mm$\leqslant \Delta X \leqslant$0.1 mm. Only a very small amount of events are left. There is at least a sharp slope at the same boundary between Fe and Ag in both the real and simulated data. This helps to verify that the alignment of X is correct. On the other hand, it shows that the position resolution does not have significant contribution to ΔX, as previously mentioned. Therefore, it cannot be used for the purpose of improving resolution without suffering dramatic statistics loss.

3.3 Extracted mixture of events

Aided by the simulation, the mixture of events after target separation could be achieved. Ignoring the gap size, a simple boundary is used, as indicated in Fig. 8 and Fig. 9, to separate the events from different targets. When this separation is applied to the simulated events, the percentage mixture from adjacent targets is obtained, as shown in Table 2.

Table 2. Events mixture in a certain target region.

mix fromRegion	Cu	Fe	Ag	Bi
Cu		0.53%		
Fe	34.6%		43.9%	
Ag		1.6%		24.13%
Bi			0.16%	

The decay time spectrum will be analyzed for events from each separated target region. For the region in which the mixture is significant, multiple lifetimes with known ratio of number of events may have to be included in fitting the decay time. For the regions in which the mixture is minor, for example less than few percent, it may be treated simply as part of the overall systematic error for the lifetime.

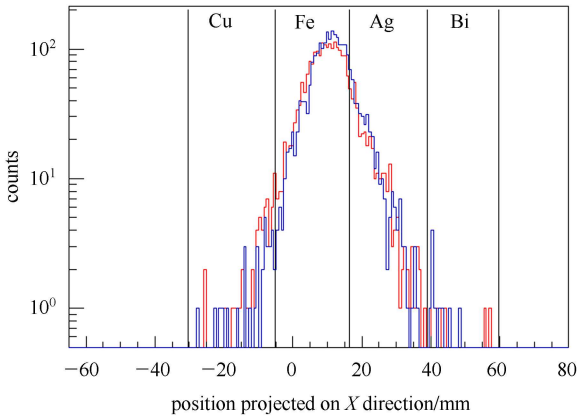

Fig. 9. (color online) The reconstructed fission position on target with an extremely tight ΔX cut: -0.1 mm$\leqslant\Delta X\leqslant$0.1 mm.

4 Summary

In this work, the concept and the technique of the JLab experiment E02-017, which aims to measure the lifetime of the heavy hypernuclei, were introduced. The crucial step in extracting the lifetime of the hypernuclei from the massive experimental data is to find the fission points on the target foil and to separate the events to the corresponding target materials. Due to limited position resolution, a substantial Monte Carlo simulation work is needed to aid the analysis. With the separated events and known mixture information, the lifetime of hypernuclei will be extracted and its final result will be reported later.

We wish to thank the technical staffers from the Accelerator Division and Hall C in Physics Division at JLab for their great support. The author Qiu Xi-Yu was also supported by the State Scholarship Fund Program of the China Scholarship Council.

References

1 Danysza M, Pniewski J. Phil. Mag., 1953, **44**: 348
2 Park H, Bhang H, Youn M et al. Phys. Rev. C, 2000, **61**: 054004
3 Ohm H, Hermes T, Borgs W, Koch H R et al. Phys. Rev. C, 1997, **55**: 3062–3065
4 Cassing W, Jarczyk L, Kamys B, Kulessa P et al. Eur. Phys. J. A, 2003, **16**: 549–561
5 Kulessa P, Rudy Z, Hartmann M, Pysz K et al. Physics Letters B, 1998, **427**: 403–408
6 Assamagan K, Baker K et al. Nucl. Instrum. Methods A, 1999, **426**: 405–419
7 SONG Yu-Shou et al. HEP & NP, 2007, **31**(08): 755–759 (in Chinese)
8 Grove R et al. Nucl. Instrum. Methods, 1970, **89**: 257–759
9 Radeka V, IEEE Trans. Nucl. Sci., 1974, **NS-21**(1): 51–70